Efficient inverted solar cells using TiO_2 nanotube arrays

2008 Nanotechnology 19 255202

(http://iopscience.iop.org/0957-4484/19/25/255202)

Nanotechnology **19** (2008) 255202 (5pp) doi:10.1088/0957-4484/19/25/255202

Efficient inverted solar cells using TiO_2 nanotube arrays

Bang-Ying Yu[1,2], Ating Tsai[3], Shu-Ping Tsai[1], Ken-Tsung Wong[2], Yang Yang[3], Chih-Wei Chu[1,5] and Jing-Jong Shyue[1,4,5]

[1] Research Center for Applied Sciences, Academia Sinica, Taipei 115, Taiwan, Republic of China
[2] Department of Chemistry, National Taiwan University, Taipei, Taiwan 106, Republic of China
[3] Department of Materials Science and Engineering, University of California Los Angeles, Los Angeles, CA 90095, USA
[4] Department of Materials Science and Engineering, National Taiwan University, Taipei, Taiwan 106, Republic of China

E-mail: gchu@gate.sinica.edu.tw and shyue@gate.sinica.edu.tw

Received 29 January 2008, in final form 15 April 2008
Published 14 May 2008
Online at stacks.iop.org/Nano/19/255202

Abstract
Using a vertical titania (TiO_2) nanotube array, an inverted polymer solar cell was constructed with power conversion efficiency up to 2.71%. In this study, self-organized TiO_2 nanotubes arrays were grown by anodizing Ti metal in glycerol electrolyte containing 0.5 wt% NH_4F and 1.0 wt% H_2O with 20 V potential. The tube length (∼100 nm) was controlled by the thickness of the sputtered titanium layer on the indium–tin oxide (ITO) substrate. The diameter of the tube was approximately 15–25 nm. After annealing in air at 500 °C for 1 h, nanotubes arrays were crystallized to the anatase phase from the initial amorphous state. Following the infiltration of polymeric semiconductor (poly(3-hexylthiophene) and (6,6)-phenyl C_{60} butyric acid methyl ester, P3HT:PCBM), the filled TiO_2 layer had an optical absorption over a range from UV to visible light. The high surface-to-volume ratio of the nanotube arrays structure increased the effective area of the active region. The high efficiency of our solar cell is attributed to the vertical TiO_2 nanotube array's enhanced conduction of photo-induced current due to its charge transport capability.

(Some figures in this article are in colour only in the electronic version)

1. Introduction

Polymer photovoltaic devices are gaining popularity due to the simple process involved in using them and the relatively low cost of silicon-based solar cells. The key of the polymer solar cell is the bulk heterojunction [1], which consists of a mixture of polymer/organic n-type and p-type semiconductors. The most common polymer photovoltaic cells are based on poly(3-hexylthiophene) (P3HT, as the p-type material) and (6,6)-phenyl C_{60} butyric acid methyl ester (PCBM, as the n-type material) [1, 2]. This interpenetrating network ensures a large interfacial contact area between the two components; hence, the charge separation capability is significantly enhanced. One of the dilemmas in this type of solar cell is the trade-off between the absorption and the charge transport of the active layer. Thicker polymer film enhances the optical absorption, but prevents the effectiveness of carrier transport due to the limited exciton diffusion length, typically in the 5–15 nm range [3]. In order to obtain a high charge separation yield, the electron acceptor must be intermixed with the polymers on the nanometer scale [4].

To overcome this limitation, the surface area of the donor–acceptor interface can be further increased by introducing functional nanostructures that help charge collection and transportation. A promising approach is to fill titania nanotube arrays films with organic semiconductors [5]. Highly ordered vertically oriented TiO_2 nanotube arrays fabricated by potentiostatic anodization offer a large internal surface

[5] Authors to whom any correspondence should be addressed.

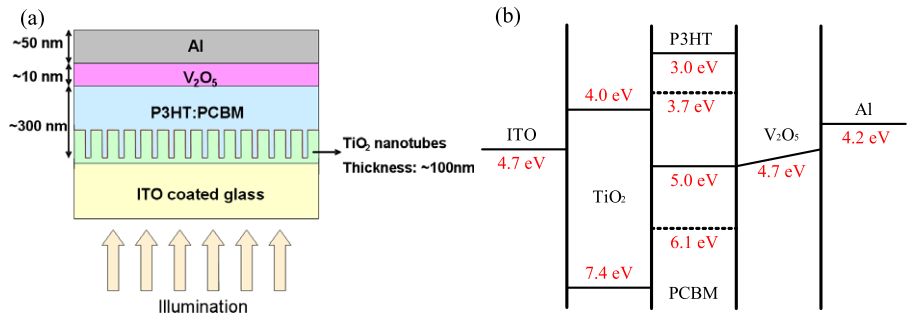

Figure 1. (a) Schematic diagram of the polymer solar cell device structure fabricated in this study. (b) Theoretical energy level diagrams for various materials in the inverted solar cells.

area, the pore size of which is typically 15–25 nm. This is comparable with the diffusion length of excitons [6, 7]. These two characteristics promote charge separation and reduce the exciton recombination. The enhancement in the electronic transportation also allows polymer solar cells with a thicker active layer, which can increase the optical density, thus improving the absorption of photons.

In this paper, we will demonstrate an enhancement in polymer solar cell efficiency by using a thick hybrid layer with P3HT:PCBM/TiO_2 nanotubes arrays up to 300 nm. The TiO_2 nanotube arrays length is about 110 nm, grown on an ITO substrate by the anodization of Ti films. The polarity of solar cells can be reversed by using a layer of transition metal oxide, such as V_2O_5, as the anodic buffer layer, independent of the top and bottom electrodes [8, 9]. An efficient inverted polymer solar cell was fabricated with the device structure ITO/TiO_2/P3HT:PCBM/V_2O_5/Al, where ITO and Al function as the cathode and anode, respectively. The schematic of device structure is shown in figure 1(a). In addition, a thin Au layer could be used as the top electrode to fabricate transparent polymer solar cells.

Based on the result, we can treat V_2O_5 as a hole injection layer with 'effective' work function of ∼5.0 eV and the TiO_2 nanotube array as an electron transport layer with a lower work function (∼4.2 eV). Both interlayers provide ohmic contacts in the heterojunction [9, 10]. The polarity of the device is decided by the relative positions of these two interfacial layers and is insensitive to the conducting electrodes. The theoretical energy level diagram for the inverted configuration is illustrated in figure 1(b).

2. Experimental methods

2.1. Titania nanotube arrays by anodization

The samples with Ti thin film on ITO substrates were cleaned by sonicating in acetone and ethanol, followed by rinsing with deionized water and drying in a nitrogen stream. TiO_2 nanotube arrays with 100 ± 10 nm length and 15 ± 5 nm pore size were then grown by anodic oxidation of 110 nm thin Ti layers sputtered on ITO substrates. The electrochemical experiments were performed using a high-voltage potentiostat (Programmable DC Power Supply, Motech). The electrolytes were 0.5 wt% NH_4F and 1.0 wt% H_2O in glycerol (1,2,3-propanetriol) [11] with a dynamic viscosity of 1350 mPa s at 20 °C, and a Pt foil was used as the counter electrode. The electrolytes were prepared from reagent-grade chemicals. The electrochemical treatment consisted of a potential ramp from the open-circuit potential (OCP) to 20 V, after which the applied potential was held at 20 V for 15–35 min.

After the electrochemical treatment, the samples were cleaned with deionized water and dried in a nitrogen stream. The initial titania nanotube arrays are well known to be amorphous. The resulting amorphous nanotube array samples were annealed in oxygen to induce crystallization and to increase the transparency [6, 11]. In this experiment, samples were heat treated at 100, 200, 300, 400 and 500 °C for 1 h, with heating and cooling rates of 5 °C min^{-1}. The microstructures of the prepared nanotube arrays were observed with a scanning electron microscope (SEM: FEI Nova200 NanoSEM, operated in the low-vacuum mode with a Helix® detector and conductive over-coats were not applied) and the crystallinity was examined with a transmission electron microscope (TEM: JEOL JEM-2100F operated at 200 kV).

2.2. Fabrication and evaluation of polymer solar cells

An active layer about 300 nm thick was spin-coated from P3HT/PCBM 1:1 weight ratio solution in dichlorobenzene (DCB) at 600 rpm for 60 s on ITO glass [12] coated with titania nanotube array prepared as described above. The hydrodynamic diameter of the blend in DCB was measured by dynamic light scattering (BIC 90Plus). The specimen was then annealed at 110 °C for 20 min. The V_2O_5 (10 nm) and anode Al (50 nm) were thermally evaporated at the rate of 0.03 and 0.3 nm s^{-1}, respectively. The Thermo-Oriel 150 W solar simulator with an AM1.5G filter provides 100 mW cm^{-2} illumination, determined by an NREL calibrated Si-detector (with a KG-5 color filter), and spectral mismatch was corrected.

3. Results and discussion

Figure 2 shows the morphology and crystalline phase of the anodized TiO_2 nanoarray on ITO before and after the heat treatment. After the heat treatment, the structural phase of the TiO_2 array transformed from the amorphous to the anatase phase. The pore diameter increased slightly and the pore density decreased after the heat treatment, indicating

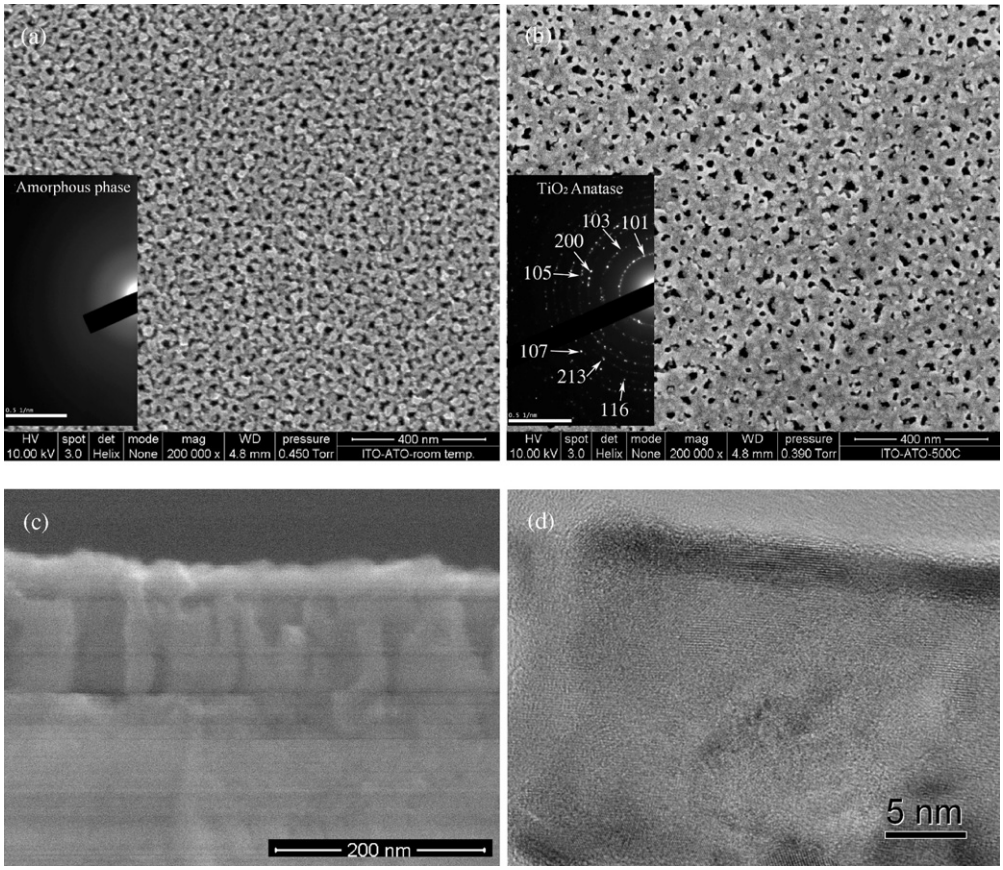

Figure 2. TiO_2 nanotube array: (a) SEM top view of sample without calcination; (b) top view and (c) cross-sectional SEM images of sample after heat treatment at 500 °C; (d) TEM lattice image of calcined nanotube arrays. The insets in (a) and (b) show the electron diffraction patterns of corresponding TiO_2 layer.

that the structure collapsed to some extent during the phase transformation.

TiO_2 nanotube arrays have been demonstrated to result in enhanced light absorption and improved charge collection efficiency as an n-type material in dye sensitized solar cells [13, 14]. Li *et al* [9] reported that the efficient polymer solar cell with inverted configuration can be fabricated by using a transition metal oxide (V_2O_5) as the anodic buffer layer. With the buffer layer, a 2.25% power conversion efficiency (PCE) was demonstrated. V_2O_5 is highly transparent and prevents the diffusion of the metal electrodes into the active organic layer while maintaining good device performance. In this work, the P3HT/PCBM blend absorbs light and carries excitons to the polymer/TiO_2 interface. The electron–hole pairs are transported to the top metal electrode through the V_2O_5 buffer, and the TiO_2 nanotube arrays accepts electrons from the conjugated polymer, and transports them to the ITO.

There are several reasons that the TiO_2 nanotube array was chosen as the electron-transporting layer to improve the photo-induced current. The nanotube arrays structure is known to possess high surface-to-volume ratio. The interface contact area can be increased by filling the TiO_2 nanotube arrays (15–25 nm pore diameter) with P3HT:PCBM blended (10–11 nm in diameter as determined by dynamic light scattering). Figure 3 shows the cross-sectional SEM image of the electrode after polymer infiltration. It is evident that the polymer was

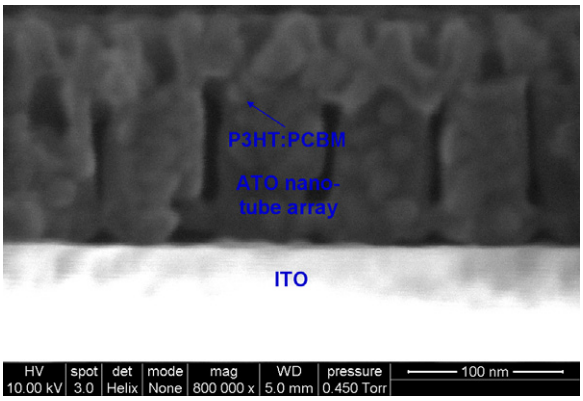

Figure 3. Cross-sectional SEM images of TiO_2 nanotube array after P3HT:PCBM infiltration.

adsorbed by the tubular motif. Consistent with the SEM image, x-ray photoelectron spectroscopy (XPS) depth-profiling found that the P3HT had partially infiltrated the tube, and a higher PCBM:P3HT ratio was observed at the bottom, suggesting that P3HT did not fully fill the tube [15].

Although P3HT has a diameter comparable to that of the nanotube arrays, the polymer could be pulled into the tube by capillary force. In this structure, charge separation can occur

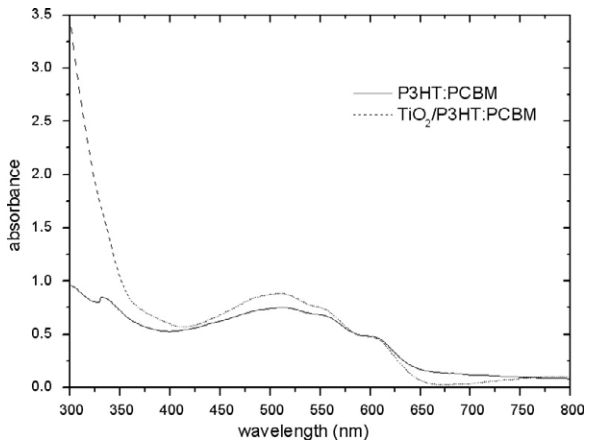

Figure 4. The absorption spectra of TiO_2 nanotube arrays infiltrated with P3HT:PCBM (broken line) and bare P3HT:PCBM film (solid line).

at the TiO_2–P3HT and PCBM–P3HT interfaces, respectively. Moreover, the nanotube arrays structure permits vertical charge transport from the active layer to the electrode. Therefore, the TiO_2 electrode is able to collect the charges more efficiently than a planar cathode structure.

Likewise, in our devices, the absorption layer is very thick (up to ∼300 nm), which improves the light absorption. The absorption spectra (figure 4) showed that the absorbance at ∼510 nm increased with the use of the TiO_2 array. This observation indicated that the amount of active layer was increased. Although the probability of exciton recombination is higher with a thicker active layer due to the small carrier mobility, this drawback can be neglected in our device because of the infiltration of the active layer into the nanotube array. In addition, the pore size of the nanotube arrays architecture of about 20 nm is comparable to the diffusion length to promote charge separation. Therefore, the current density (J_{sc}, discussed below) is increased 30% compared to that in the previous work done by Li *et al* with a similar inverted structure [9].

Current–voltage (I–V) characteristics of photovoltaic devices with TiO_2 annealed at different temperatures are compared in figure 5(a). The anodization time for forming the TiO_2 nanotube arrays was 30 min, and the samples were placed in the furnace at 100, 200, 300, 400 and 500 °C for 1 h with heating and cooling rates of 5 °C min^{-1}. The device annealed at 500 °C exhibited a significant improvement in the photovoltaic performance compared with those devices annealed at lower temperatures. Under AM1.5G with 100 mW cm^{-2} illumination, the best device, with 500 °C annealing, showed a short-circuit current density (J_{sc}) of 9.33 mA cm^{-2}, an open-circuit voltage (V_{oc}) of 0.59 V, and a fill factor (FF) of 48%, resulting in a power conversion efficiency of 2.65%.

The PCE degraded rapidly to 1.18% when the annealing temperature was decreased to 400 °C. At low annealing temperatures such as RT and 100 °C, the short-circuit currents (I_{sc}) were almost two orders of magnitude less compared to the values obtained with an annealing temperature of 500 °C. This result is consistent with enhanced crystallinity after heat treatment. In other words, the device with TiO_2 nanotubes arrays heated up to 500 °C had better crystallization and resulted in higher current density. Further increase in the annealing temperature would have been a disadvantage as the conductivity of ITO decreases [16]. In addition the phase transformation from anatase to rutile could take place at high temperature [17].

Figure 5(b) shows the I–V characteristics with different anodization time of the titanium thin film. As the anodization time increases, the TiO_2 nanotube arrays structure is more developed and the portion of thin film decreases. As a consequence of the results reported in the previous section, we annealed all the samples up to 500 °C to induce the crystallinity of the TiO_2 nanotubes arrays. The sample without anodization showed extremely small J_{sc} due to the large resistance of the dense TiO_2 layer preventing the layer from being an electron-transporting material. TiO_2 nanotube arrays formed by anodizing for 27 and 30 min showed good performances, with PCE of 2.71% and 2.65%, respectively. However, the PCE dropped significantly for specimens that were anodized for 35 min. The reason is that if the Ti is anodized for less than 27 min, the charge collection will not have become efficient due to the incomplete nanotube arrays. In this case, the residual Ti metal oxidized into TiO_2 thin film after subsequent heat treatment, and the structureless thin film increased the series resistance in the cell.

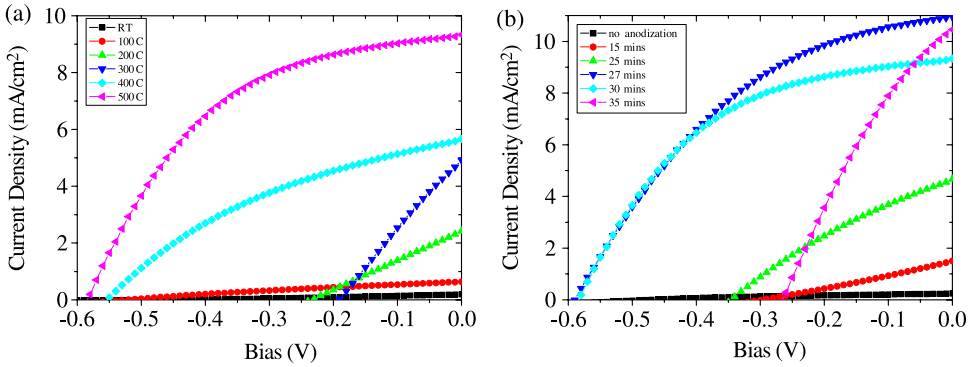

Figure 5. I–V characters of polymer photovoltaic device with (a) different TiO_2 annealing temperature and (b) different anodization time of titanium thin film.

For a longer time of anodization (35 min), the Ti layer is over anodized. Therefore, the electrolyte contacted the ITO substrate directly, and the ITO was etched by the weak-acid electrolyte. SEM investigation of the sample anodized for 35 min confirmed that the ITO was etched, resulting in voids, which degraded the performances of the devices due to the degradation of the contact and conductivity. Therefore, the anodization time is an important factor in fabricating an efficient polymer solar cell.

4. Conclusion

In conclusion, applying a thin layer of vertically oriented TiO_2 nanotube arrays on an ITO substrate with an inverted architecture for charge generation and collection in heterojunction solar cells with high efficiency was presented in this work. A blend of regioregular poly(3-hexylthiophene) (P3HT) and [6, 6]-phenyl C_{60} butyric acid methyl ester (PCBM) was infiltrated into a 100 nm optically transparent TiO_2 nanotube array. Both the P3HT–TiO_2 and P3HT–PCBM provide interfaces for charge separation, and the TiO_2 nanotubes arrays permit vertical charge transport from the absorption layer to the electrode. With the TiO_2 electrode prepared by anodizing a 100 nm thick Ti film on ITO for 27 min at 20 V and then annealing at 500 °C for 1 h, the resulting polymer solar cells show a short-circuit current density of 10.96 mA cm^{-2}, and 0.59 V open-circuit potential, and a 0.42 fill factor, yielding a power conversion efficiency of 2.71%.

Acknowledgments

This research was sponsored by the Academia Sinica and the Taiwan National Science Council through Grant Numbers 96-2120-M-002-018 and 96-2221-E-001-017-MY2.

References

[1] Yu G, Gao J, Hummelen J C, Wudl F and Heeger A J 1995 *Science* **270** 1789–91
[2] Takanezawa K, Hirota K, Wei Q-S, Tajima K and Hashimoto K 2007 *J. Phys. Chem.* C **111** 7218–23
[3] Dennler G and Sariciftci N S 2005 *Proc. IEEE* **8** 1432
[4] Coakley K M and McGehee M D 2003 *Appl. Phys. Lett.* **83** 3380–2
[5] Mor G K, Varghese O K, Paulose M, Shankar K and Grimes C A 2006 *Sol. Energy Mater. Sol. Cells* **90** 2011–75
[6] Paulose M, Shankar K, Varghese O K, Mor G K and Grimes C A 2006 *J. Phys. D: Appl. Phys.* **39** 2498–503
[7] Shankar K, Mor G K, Prakasam H E, Yoriya S, Paulose M, Varghese O K and Grimes C A 2007 *Nanotechnology* **18** 065707
[8] Shrotriya V, Li G, Yao Y, Chu C-W and Yang Y 2006 *Appl. Phys. Lett.* **88** 073508
[9] Li G, Chu C-W, Shrotriya V, Huang J and Yang Y 2006 *Appl. Phys. Lett.* **88** 253503
[10] Kim J Y, Kim S H, Lee H H, Lee K, Ma W L, Gong X and Heeger A J 2006 *Adv. Mater.* **18** 572
[11] Mor G K, Varghese O K, Paulose M and Grimes C A 2005 *Adv. Funct. Mater.* **15** 1291
[12] Kim J Y, Kim S H, Lee H H, Lee K, Ma W, Gong X and Heeger A J 2006 *Adv. Mater.* **18** 572
[13] Ong K G, Varghese O K, Mor G K, Shankar K and Grimes C A 2007 *Sol. Energy Mater. Sol. Cells* **91** 250
[14] Mor G K, Shankar K, Paulose M, Varghese O K and Grimes C A 2007 *Appl. Phys. Lett.* **91** 152111
[15] Yu B-Y, Chen Y-Y, Wang W-B, Hsu M-F, Tsai S-P, Lin W-C, Lin Y-C, Jou J-H, Chu C-W and Shyue J-J 2008 *Anal. Chem.* ASAP article http://pubs.acs.org/cgi-bin/abstract.cgi/ancham/asap/abs/ac702626n.html
[16] Ryzhikov I A, Pukhov A A, Il'in A S, Glukhova N P, Afanasiev K N and Ryzhikov A S 2003 *Microelectron. Eng.* **69** 270
[17] Li J-G and Ishigaki T 2004 *Acta Mater.* **52** 5143–50